

Nearly free electron model and k-p method calculations of electronic band structure of wurtzite InN

Kejia Wang* and Debdeep Jena†

Department of Electrical Engineering, University of Notre Dame, IN, 46556, USA

(Dated: December 12, 2006)

The theoretical models for calculations of band structure of wurtzite InN have been studied. Several models including nearly free electron model, pseudopotential method, Tight-Binding method and k-p method will be discussed. Currently most InN epitaxial films grown on GaN or sapphire substrate have wurtzite structure. To study the symmetry properties of the electron wave function in wurtzite structure, a nearly free electron model calculation for GaN and InN are shown. Based on that, band structure calculated using k-p method near Γ point will be presented.

INTRODUCTION

Indium nitride, as the least studied semiconductor in nitrides family (AlN-GaN-InN), has attracted much interests in recent years. The most interesting and controversially property is the fundamental bandgap of InN. Before 2003, the InN films was mainly grown by sputter techniques and the accepted bandgap measured from absorption edge was around 1.9 eV [1, 2]. Recently high quality InN epitaxial films have been grown by both metal organic chemical vapor deposition (MOCVD) [3, 4] and Molecular Beam Epitaxy (MBE) [5-8], the optical characterizations including photoluminescence and absorption spectrum show that the bandgap of InN is around 0.7 eV [6, 9, 10], which is much smaller than previously reported value. And it is also found that there is no noticeable feature around 1.9 eV.

The origin of this big discrepancy has been explained in many hypotheses. Since InN has a high electron affinity, almost all impurities and defects will act as donors, and thus result in high electron concentration in InN [11]. Even in unintentionally doped InN, the electron concentration was observed in the order of $\times 10^{17} \sim \times 10^{18} \text{ cm}^{-3}$ [5, 6]. And the Fermi level in InN was believed to be inside the conduction band, and about 180 meV above conduction band edge [12]. This high Fermi level could produce the Burstein-Moss shift, which results in blue shift in absorption edge. Wu et. al has shown that the absorption edge increased with the increasing of electron concentration [13]. The formation of oxidation and precipitation of In clusters could also effect the optical properties of InN [14, 15].

The narrow bandgap of InN opens many opportunities for the application of opto-electronic devices in IR region and high speed electronic devices [16, 17]. InN and high indium composition InGaN could be possible materials for opto-electronic devices IR regions for communication applications. Since the nitrides (AlN, GaN and InN) semiconductor bandgap energy can cover the whole solar spectrum, they can be used for high efficiency photovoltaic application with environment friendly non-toxic elements. Due to the narrow bandgap of InN, a

small effective electron mass ($0.05m_0$) has been assigned to InN [18]. As a result, high electron mobility of $14000 \text{ cm}^2/\text{V}\cdot\text{s}$ at room temperature has been predicted by a Monte-Carlo simulation [19]. Thus InN is very attractive for high speed electronic devices. Leary et al. have used a three-valley Monte-Carlo simulate to analysis the steady state and transient electron transport properties in InN [20]. They found that the drift velocity was greatly depends on the band structure such as the bandgap, effective mass and non-parabolic coefficient. Thus to fully understand the band structure of InN is very important to explore its electrical and optical properties and also device performance.

So far many investigations have been carried out on calculating the band structure of InN. Before 2003, due to lack of basic parameters of InN, early theoretical calculations using empirical pseudopotential model predicted the bandgap of wurtzite InN was around $2.0 \sim 2.6 \text{ eV}$ [21-23]. One year later, the same group using new InN parameters had calculated the bandgap of 0.79 eV and the electron effective mass of $0.07m_0$ [24]. Recently, many works have been done using the first principle calculation [25] and *ab initio* calculation [26, 27]. These first-principle pseudopotential method (also known as *ab initio* method) are *self-consistent*: first an atomic pseudopotential and an ionic potential of crystal structure were used as the starting point; then wave functions have been calculated; after that the total one-electron potential was derived from the wave functions and compared with the initial potential. On the other hand, empirical pseudopotential requires experimental inputs such as atomic pseudopotential form factor. However the atomic pseudopotential form factor for one element is *transferable*, which means the atomic pseudopotential form factor of In determined from InP could be used in other In compounds such as InN and InAs. With accurate input, the empirical pseudopotential could give good overall agreement with experimental results. Other calculation like tight-binding method has also been used for band structure of nitrides [28].

Other than pseudopotential and tight-binding methods, k-p method can also to used to extrapolate $E-k$ dis-

persion relation. Compare to pseudopotential and tight-binding methods, k-p requires more experimental input data but provide more accurate results especially near the high symmetric points in Brillouin zone. Beresford has presented full-zone k-p band structure calculation of wurtzite semiconductors [29], but the author still used the old parameters for InN and got bandgap of InN to be 1.9 eV. Recently, some key parameters of InN have been extracted using density-function theory [30], which would be helpful to calculate the band structure of InN using k-p method.

In this work we present the theoretical approaching of calculation of electronic band structure of wurtzite InN. The first step was calculate the nearly free electron band (also called empty lattice model) in wurtzite structure and then use k-p method to calculate InN band structure near Γ point.

NEARLY FREE ELECTRON MODEL

In the nearly free electron model, the crystal potential is assumed to be vanishingly small. The electron energy band is simply a parabolical dispersion plotted in the reduce zone. From free electron energy equation, replace the wavevector ' k_0 ' by ' $G+k$ ', where ' k ' is the wavevector in the first Brillouin zone, the $E - k$ relation thus becomes:

$$E = \frac{\hbar^2 k_0^2}{2m} = \frac{\hbar^2}{2m}(k + G)^2, \quad (1)$$

$$E = \frac{\hbar^2}{2m}((k_x + G_x)^2 + (k_y + G_y)^2 + (k_z + G_z)^2), \quad (2)$$

where G is the reciprocal lattice point.

Equation 2 can be expanded for all the reciprocal lattice points. For each reciprocal lattice point, there will be a electron band. Table I has listed the expansion up to 19 bands. However because of the symmetry of the crystal, many bands could be degenerated and merged together. For wurtzite structure, the Brillouin Zone is shown in Figure 1. The full band structure will be plot in the following sequence: $\Gamma \rightarrow A \rightarrow H \rightarrow K \rightarrow \Gamma \rightarrow M \rightarrow U \rightarrow A$ (Figure 1b).

Eventhough this nearly free electron approach doesn't consider any crystal structure, it still looks very similar to other large-scale numerical calculation such as tight-binding and pseudopotential methods. Figure 2 shows the calculation of GaN band structure and compared with near free electron model calculation. Since the nearly free electron model doesn't consider the crystal potential, so there is no energy split at high symmetry points and thus no bandgaps have been shown. Away from those high symmetry points, the shape of electron

TABLE I: Near free electron band structure calculation.

Band	G vector	$(k_x + G_x)^2$	$(k_y + G_y)^2$	$(k_z + G_z)^2$
1	(000)	k_x^2	k_y^2	k_z^2
2	(100)	$(k_x + G_x)^2$	k_y^2	k_z^2
3	($\bar{1}$ 00)	$(k_x - G_x)^2$	k_y^2	k_z^2
4	(010)	k_x^2	$(k_y + G_y)^2$	k_z^2
5	(0 $\bar{1}$ 0)	k_x^2	$(k_y - G_y)^2$	k_z^2
6	(001)	k_x^2	k_y^2	$(k_z + G_z)^2$
7	(00 $\bar{1}$)	k_x^2	k_y^2	$(k_z - G_z)^2$
8	(110)	$(k_x + G_x)^2$	$(k_y + G_y)^2$	k_z^2
9	(101)	$(k_x + G_x)^2$	k_y^2	$(k_z + G_z)^2$
10	($\bar{1}$ 10)	$(k_x + G_x)^2$	$(k_y - G_y)^2$	k_z^2
11	(10 $\bar{1}$)	$(k_x + G_x)^2$	k_y^2	$(k_z - G_z)^2$
12	($\bar{1}$ 10)	$(k_x - G_x)^2$	$(k_y + G_y)^2$	k_z^2
13	(101)	$(k_x - G_x)^2$	k_y^2	$(k_z + G_z)^2$
14	($\bar{1}$ 10)	$(k_x - G_x)^2$	$(k_y - G_y)^2$	k_z^2
15	(10 $\bar{1}$)	$(k_x - G_x)^2$	k_y^2	$(k_z - G_z)^2$
16	(011)	k_x^2	$(k_y + G_y)^2$	$(k_z + G_z)^2$
17	(0 $\bar{1}$ 1)	k_x^2	$(k_y - G_y)^2$	$(k_z + G_z)^2$
18	(01 $\bar{1}$)	k_x^2	$(k_y + G_y)^2$	$(k_z - G_z)^2$
19	(0 $\bar{1}$ 1)	k_x^2	$(k_y - G_y)^2$	$(k_z - G_z)^2$

dispersion in nearly free electron model is very similar to real electron dispersion in crystal. The main reason is that away from high symmetry points, the electrons are less affected by crystal potentials and thus behave like free electrons. Figure 3a shows the InN band structure calculated from empirical pseudopotential method (EPM) [29], which predicts the energy bandgap of InN to be around 0.7 eV. Figure 3b shows the band dispersion calculated from nearly free electron model of wurtzite InN. This is very similar to that of GaN because InN and GaN have the same lattice symmetry and the only difference is the lattice constance.

K-P METHOD

The k-p method has become one of the most widely used band structure models for describing not only 3-dimensional semiconductors, but also 2-dimensional quantum well and 1-dimensional quantum wire. It was very accurate near the bandedges. However compared with Tight-binding and pseudopotential methods, k-p method requires more input datas. It starts with a bandedge calculated from tight-binding or pseudopotential methods, and then use perturbation theory to describe the bands away from the bandedge.

First, consider the time-independent Schrodinger equation:

$$H_0 \Phi_n(r) = E_n \Phi_n(r), H_0 = \frac{p^2}{2m_0} + V(r). \quad (3)$$

The Bloch theorem in reduce zone is:

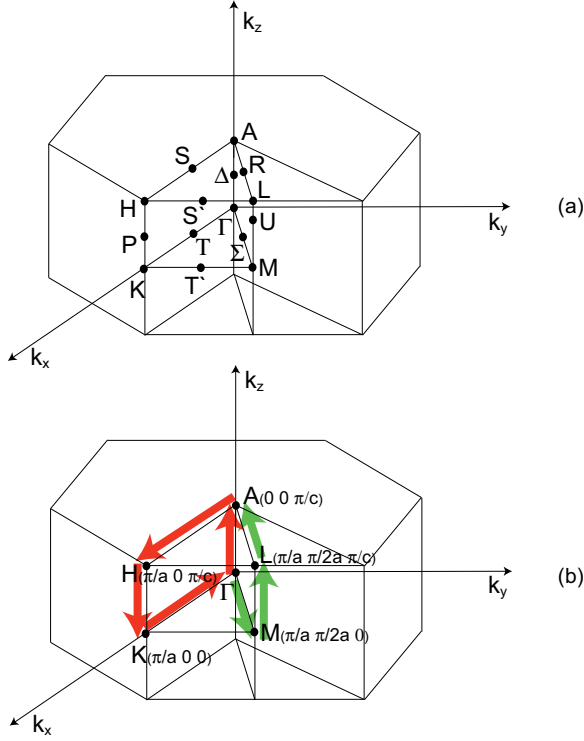


FIG. 1: (a) Brillouin zone of wurtzite InN and its high symmetry points. (b) The band structure will be plotted in the sequence of: $\Gamma \rightarrow A \rightarrow H \rightarrow K \rightarrow \Gamma \rightarrow M \rightarrow L \rightarrow A$.

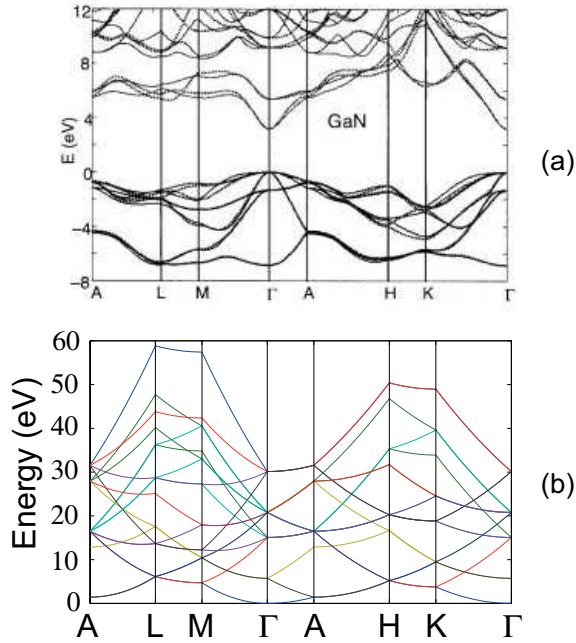


FIG. 2: (a) GaN band structure calculated from Full zone k-p method [29]. (b) Nearly free electron model calculation for electrons in wurtzite GaN.

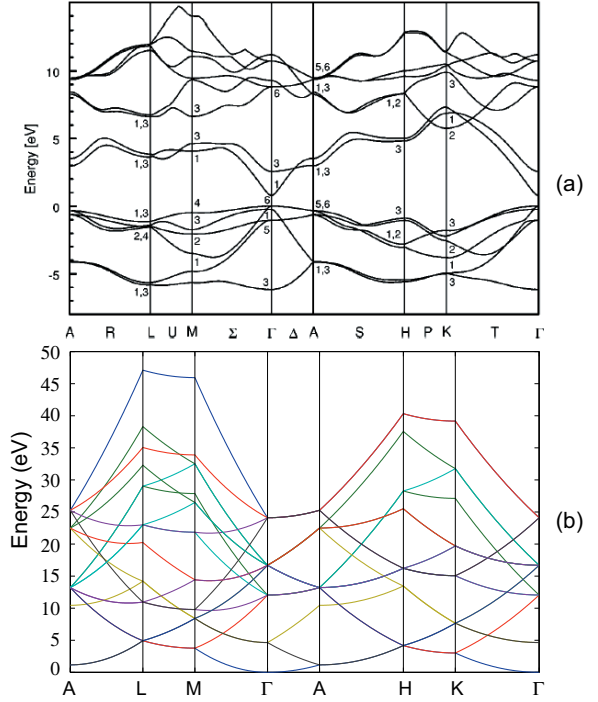


FIG. 3: (a) InN band structure calculated from empirical pseudopotential method [24]. (b) Nearly free electron model calculation for electrons in wurtzite InN.

$$\Phi_{nk} = \exp(i\mathbf{k} \cdot \mathbf{p}) u_{nk}(r). \quad (4)$$

where $u_{nk}(r)$ is the Bloch wavefunction and has the periodicity of the lattice. Suppose eigenvalue and eigenfunction near $k = k_0$ are known:

$$\left(\frac{p^2}{2m} + V(r)\right)\Phi_{nk} = E_{nk}\Phi_{nk}, \quad (5)$$

We can expand the general solutions away from the $k = k_0$ solutions in the basis set $\exp[i(k - k_0)r]$:

$$\Phi_{k,r} = \sum_n b_n(k) \psi_n(k_0, r) e^{i(k-k_0) \cdot r}, \quad (6)$$

where b_n are the expansion coefficients. Since $\mathbf{p} = -i\hbar\nabla$, so we can have:

$$\nabla(e^{i(k-k_0) \cdot r} \psi_n) = \psi_n e^{i(k-k_0) \cdot r} (\nabla + i(k - k_0)) \psi_n. \quad (7)$$

So the LHS of equation 5 becomes:

$$\left(\frac{p^2}{2m} + V(r)\right) e^{i(k-k_0) \cdot r} \psi_n$$

$$\begin{aligned}
&= e^{i(k-k_0)\cdot r} \cdot r \left[\frac{p + \hbar(k-k_0)^2}{2m_0} + V(r) \right] \psi_n \\
&= e^{i(k-k_0)\cdot r} \left[\frac{\hbar^2}{2m_0} (k-k_0)^2 + \frac{\hbar}{m_0} (k-k_0) \cdot p \right. \\
&\quad \left. + E_n \right] \psi_n. \tag{8}
\end{aligned}$$

For simplicity, consider here the Γ point: $k_0 = (000)$, equation 8 reduces to:

$$\left(\frac{p^2}{2m_0} + V + \frac{\hbar}{m} \mathbf{k} \cdot \mathbf{p} + \frac{\hbar^2 k^2}{2m_0} \right) u_{n\mathbf{k}} = E_{n\mathbf{k}} u_{n\mathbf{k}}. \tag{9}$$

The first and second terms corresponding to original Hamiltonian. The third term is the first order perturbation in k and the fourth term is the second order perturbation in k . Using Kane's model [31], Chuang and Chang had derived the 8×8 Hamiltonian for the wurtzite crystal structure [32]:

$$H_{8 \times 8} = \frac{\hbar^2 k^2}{2m_0} + \begin{bmatrix} E_c & -\frac{k_+ P_2}{\sqrt{2}} & \frac{k_- P_2}{\sqrt{2}} & k_z P_1 & 0 & 0 & 0 & 0 \\ -\frac{k_- P_2}{\sqrt{2}} & E_v + \Delta_1 + \Delta_2 & 0 & 0 & 0 & 0 & 0 & 0 \\ \frac{k_+ P_2}{\sqrt{2}} & 0 & E_v + \Delta_1 - \Delta_2 & 0 & 0 & 0 & 0 & \sqrt{2} \Delta_3 \\ k_z P_1 & 0 & 0 & E_v & 0 & 0 & \sqrt{2} \Delta_3 & 0 \\ 0 & 0 & 0 & 0 & E_c & \frac{k_- P_2}{\sqrt{2}} & -\frac{k_+ P_2}{\sqrt{2}} & k_z P_1 \\ 0 & 0 & 0 & 0 & \frac{k_+ P_2}{\sqrt{2}} & E_v + \Delta_1 + \Delta_2 & 0 & 0 \\ 0 & 0 & 0 & \sqrt{2} \Delta_3 & -\frac{k_- P_2}{\sqrt{2}} & 0 & E_v + \Delta_1 - \Delta_2 & 0 \\ 0 & 0 & \sqrt{2} \Delta_3 & 0 & k_z P_1 & 0 & 0 & E_v \end{bmatrix}, \tag{10}$$

where

$$k_{\pm} = k_x \pm ik_y, \tag{11}$$

and Δ_1 is related to the crystal field split energy Δ_{cr} , and Δ_2 and Δ_3 are related to the spin-orbit split-off energy Δ_{so} by:

$$\Delta_1 = \Delta_{cr}, \Delta_2 = \Delta_3 = \frac{1}{3} \Delta_{so}. \tag{12}$$

P_1 and P_2 are Kane's parameters:

$$P_1^2 = \frac{\hbar^2}{2m_0} \left(\frac{m_0}{m_e^z} - 1 \right) \frac{(E_g + \Delta_1 + \Delta_2)(E_g + 2\Delta_2) - 2\Delta_3^2}{E_g + 2\Delta_2}, \tag{13}$$

and

$$P_2^2 = \frac{\hbar^2}{2m_0} \left(\frac{m_0}{m_e^z} - 1 \right) \frac{E_g [(E_g + \Delta_1 + \Delta_2)(E_g + 2\Delta_2) - 2\Delta_3^2]}{(E_g + \Delta_1 + \Delta_2)(E_g + 2\Delta_2) - \Delta_3^2}, \tag{14}$$

where m_e^t is the transverse effective mass (in $x-y$ plane) and m_e^z is the longitudinal effective mass (in z direction). Solving Hamiltonian of equation 10 for little

TABLE II: InN parameters used in simulation from Ref. [24, 30]

Parameter	m_e^t	m_e^z	Δ_{cr}	Δ_{so}	E_g
Unit	m_0	m_0	meV	meV	eV
wz-InN	0.071	0.067	17	3	0.65

perturbation of k near Γ could give corresponding eigenvalues and thus get $E-k$ dispersion near band edge.

Parameters used in this work are listed in Table II. Using $k \cdot p$ method, the band dispersions near Γ point along k_x , k_y , and k_z directions are plotted in Figure 4. Figure 5 (a) shows the conduction bands along different directions. Due to the symmetry, $E-k$ dispersions are identically same along k_x and k_y . InN has smaller effective mass along k_z directions than k_x and k_y . Before 2003, the bandgap of InN was believed to be around 1.9 eV with larger effective mass. Figure 5 (b) shows the simulations using new InN parameters and old InN parameters. Due to the narrower bandgap, smaller electron effective mass should be assigned.

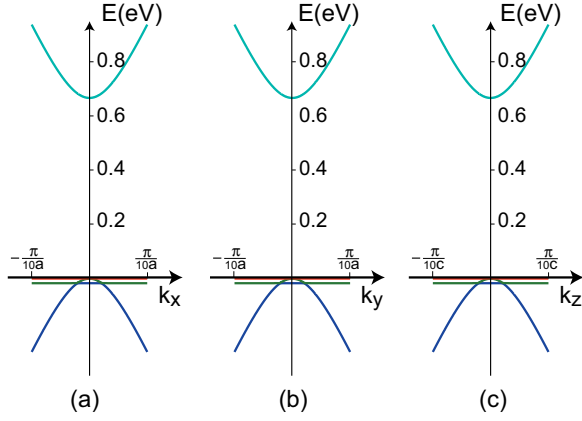


FIG. 4: InN $E - k$ dispersion plotted near Γ point along (a) k_x , (b) k_y , (c) k_z directions.

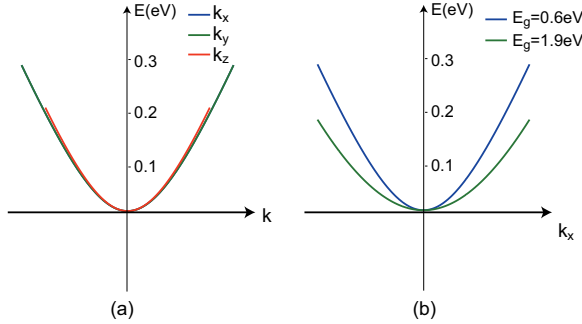


FIG. 5: (a) Comparison of conduction band dispersion along k_x , k_y , and k_z directions. (b) Comparison of conduction band dispersion along k_x direction for InN with bandgap of 0.65 eV and 1.9 eV. Parameters for InN with 1.9 eV are from Ref. [23]

CONCLUSION

In summary, we have presented the details of nearly free electron model and k-p method. Full band dispersion relationship has been derived using nearly free electron model for wurtzite GaN and InN. The results have been compared with other band structure simulations such as pseudopotential and k-p methods. It can be shown that nearly free electron model could highlight the symmetry of the crystal structure and predict the shape of the band dispersion away from high symmetry points. Furthermore, using a 8×8 Hamiltonian from Kane's model, band dispersion relations have been calculated near Γ point using new InN parameters.

* Electronic mail: kwang@nd.edu

† Electronic mail: djena@nd.edu

[1] T. L. Tansley and C. P. Foley, J. of Appl. Phys. **59**, 3241

- (1986).
- [2] W. Z. Shen, L. F. Jiang, H. F. Yang, F. Y. Meng, H. Ogawa, and Q. X. Guo, Appl. Phys. Lett. **80**, 2063 (2002).
- [3] A. Yamamoto, T. Tanaka, K. Koide, and A. Hashimoto, phys. stat. sol. (b) **194**, 510 (2002).
- [4] R. S. Q. Fareed, R. Jain, R. Gaska, M. S. Shur, J. Wu, W. Walukiewicz, and M. A. Khan, Appl. Phys. Lett. **84**, 1892 (2004).
- [5] H. Lu, W. J. Schaff, J. Hwang, H. Wu, G. Koley, and L. F. Eastman, Appl. Phys. Lett. **79**, 1489 (2001).
- [6] Y. Nanishi, Y. Saito, and T. Yamaguchi, Jpn. J. Appl. Phys. **42**, 2549 (2003).
- [7] E. Dimakis, E. Iliopoulos, K. Tsagaraki, T. Kehagias, P. Komninou, and A. Georgakilas, J. of Appl. Phys. **97**, 113520 (pages 10) (2005).
- [8] C. S. Gallinat, G. Koblmuller, J. S. Brown, S. Bernardis, J. S. Speck, G. D. Chern, E. D. Readinger, H. Shen, and M. Wraback, Appl. Phys. Lett. **89**, 032109 (pages 3) (2006).
- [9] J. Wu, W. Walukiewicz, K. M. Yu, J. W. A. III, E. E. Haller, H. Lu, W. J. Schaff, Y. Saito, and Y. Nanishi, Appl. Phys. Lett. **80**, 3967 (2002).
- [10] J. Wu, W. Walukiewicz, S. X. Li, R. Armitage, J. C. Ho, E. R. Weber, E. E. Haller, H. Lu, W. J. Schaff, A. Barcz, et al., Appl. Phys. Lett. **84**, 2805 (2004).
- [11] J. Wu and W. Walukiewicz, Superlatt. Microstruct. **34**, 63 (2003).
- [12] K. A. Wang, Y. Cao, J. Simon, J. Zhang, A. Mintairov, J. Merz, D. Hall, T. Kosel, and D. Jena, Appl. Phys. Lett. **89**, 162110 (pages 3) (2006).
- [13] J. Wu, W. Walukiewicz, W. Shan, K. M. Yu, J. W. Ager, E. E. Haller, H. Lu, and W. J. Schaff, Phys. Rev. B **66**, 201403 (2002).
- [14] K. Butcher and T. Tansley, Superlattices Microstruct. **38**, 1 (2005).
- [15] W. Walukiewicz, J. W. A. III, K. M. Yu, Z. Liliental-Weber, J. Wu, S. X. Li, R. E. Jones, and J. D. Denlinger, J. Phys. D **39**, R83 (2006).
- [16] S. K. O'Leary, B. E. Foutz, M. S. Shur, and L. F. Eastman, Appl. Phys. Lett. **88**, 152113 (pages 3) (2006).
- [17] M. Kurouchi, H. Naoi, T. Araki, T. Miyajima, and Y. Nanishi, Jpn. J. Appl. Phys. **44**, L230 (2005).
- [18] S. P. Fu and Y. F. Chen, Appl. Phys. Lett. **85**, 1523 (2004).
- [19] V. M. Polyakov and F. Schwierz, Appl. Phys. Lett. **88**, 032101 (pages 3) (2006).
- [20] S. K. O'Leary, B. E. Foutz, M. S. Shur, and L. F. Eastman, Appl. Phys. Lett. **87**, 222103 (pages 3) (2005).
- [21] C. P. Foley and T. L. Tansley, Phys. Rev. B **33**, 1430 (1986).
- [22] Y. C. Yeo, T. C. Chong, and M. F. Li, J. Appl. Phys. **83**, 1429 (1998).
- [23] D. Fritsch, H. Schmidt, and M. Grundmann, Phys. Rev. B **67**, 235205 (pages 13) (2003).
- [24] D. Fritsch, H. Schmidt, and M. Grundmann, Physical Review B (Condensed Matter and Materials Physics) **69**, 165204 (pages 5) (2004).
- [25] C. K. Gan and D. J. Srolovitz, Phys. Rev. B **74**, 115319 (pages 5) (2006).
- [26] F. Bechstedt and J. Furthmueller, J. Cryst. Growth **246**, 315 (2002).
- [27] D. Bagayoko and L. Franklin, J. Appl. Phys. **97**, 123708 (pages 5) (2005).

- [28] J.-M. Jancu, F. Bassani, F. D. Sala, and R. Scholz, *Applied Physics Letters* **81**, 4838 (2002).
- [29] R. Beresford, *J. Appl. Phys.* **95**, 6216 (2004).
- [30] P. Rinke, M. Scheffler, A. Qteish, M. Winkelnkemper, D. Bimberg, and J. Neugebauer, *Appl. Phys. Lett.* **89**, 161919 (pages 3) (2006).
- [31] E. O. Kane, *J. Phys. Chem. Solidi* **1**, 249 (1957).
- [32] S. L. Chuang and C. S. Chang, *Phys. Rev. B* **54**, 2491 (1996).